Long noncoding RNA SH3PXD2A-AS1 promotes NSCLC proliferation and accelerates cell cycle progression by interacting with DHX9

Yeqing Zhou
Xuzhou Medical University
Hongmei Yong
Affiliated Huai'an Hosptial of Xuzhou Medical University
Sufang Chu
Xuzhou Medical University
Minle Li
Xuzhou Medical University
Zhongwei Li
Xuzhou Medical University
Jin Bai
Xuzhou Medical University
Hao Zhang (zhanghao@xzhmu.edu.cn)
Affiliated Hospital of Xuzhou Medical University https://orcid.org/0000-0002-2926-737X

Research Article

Keywords: SH3PXD2A-AS1, NSCLC, FOXM1, DHX9, Cell cycle

Posted Date: March 11th, 2021

DOI: https://doi.org/10.21203/rs.3.rs-280145/v1

Version of Record: A version of this preprint was published at Cell Death Discovery on April 11th, 2022.
See the published version at https://doi.org/10.1038/s41420-022-01004-6.

Abstract

Background

As the most commonly diagnosed lung cancer, non–small cell lung carcinoma (NSCLC) is regulated by many long noncoding RNAs (lncRNAs). In the present study, we found that SH3PXD2A-AS1 expression in NSCLC tissues was upregulated compared with that in normal lung tissues in The Cancer Genome Atlas (TCGA) database. However, the role and molecular mechanism of SH3PXD2A-AS1 in NSCLC progression require further exploration.

Methods

The expression of SH3PXD2A-AS1 in NSCLC and normal lung tissues in a TCGA dataset was analysed by using the GEPIA website. K-M analysis was performed to explore the effects of this molecule on the survival rate in NSCLC. The functional characterization of the role and molecular mechanism of SH3PXD2A-AS1 in NSCLC was performed with a series of in vitro and in vivo experiments.

Results

SH3PXD2A-AS1 expression was increased in human NSCLC, and high SH3PXD2A-AS1 expression was correlated with poor overall survival. SH3PXD2A-AS1 overexpression sufficiently promoted tumour cell proliferation and accelerated cell cycle progression in vitro and tumour growth in vivo. Moreover, SH3PXD2A-AS1 interacted with DHX9 to enhance FOXM1 expression, promote tumour cell proliferation and accelerate cell cycle progression.

Conclusions

SH3PXD2A-AS1 promoted NSCLC growth by interacting with DHX9 to enhance FOXM1 expression. SH3PXD2A-AS1 may serve as a promising predictive biomarker for the diagnosis and prognosis of patients with NSCLC.

Background

Lung cancer is one of the most commonly diagnosed cancers and the most frequent cause of cancer-related death globally [1]. Approximately 85% of all new lung cancer cases are non–small cell lung carcinoma (NSCLC). Although many advances have been made in recent years, the issue of diagnosis at advanced stages and the propensity for metastasis still result in poor outcomes, and the overall 5-year survival rate for the disease is less than 15% [2, 3]. Thus, identification of novel effective biomarkers for early diagnosis, prognosis and therapeutic improvement is urgently needed.

Long noncoding RNAs (lncRNAs) are an important group of transcribed RNA molecules greater than 200 nucleotides in length with no or limited protein coding capability [4, 5]. LncRNAs participate in multiple biological processes in cancer cells, and the dysregulation of lncRNAs is highly associated with cancer cell proliferation, energy metabolism, invasion and metastasis through mechanisms at the transcriptional or post-transcriptional level [6–8]. For example, the long noncoding RNA GMAN, which is upregulated in gastric cancer tissues, is associated with migration and metastasis [9]. LncRNA KTN1-AS1 predicts a poor prognosis and regulates non–small cell lung cancer cell proliferation [10]. LncRNAs may be important regulators of tumorigenesis and proliferation [11–13], but the detailed mechanisms of lncRNAs in lung cancer should be further elucidated. These results prompted us to explore the role of lncRNAs in human NSCLC.

In a preliminary experiment, we assayed SH3PXD2A-AS1 expression through The Cancer Genome Atlas (TCGA) database in NSCLC; we detected higher expression in tumour tissues than in normal tissues and found that high expression was associated with a poor prognosis. SH3PXD2A-AS1 is an antisense transcript transcribed from SH3PXD2A and located on chromosome 10 and is 2023 bp in length. SH3PXD2A-AS1 has recently been reported to be upregulated in CRC tissues and to promote cell proliferation, cell cycle progression, migration and invasion [14, 15]. However, its biological role and specific mechanism in NSCLC should be further uncovered.

To further elucidate the mechanism by which SH3PXD2A-AS1 regulates lung cancer, we identified probable target genes of SH3PXD2A-AS1 in NSCLC. Forkhead box M1 (FOXM1), also known as HNF-3, HFH-11 or Trident, is a transcription factor of the Forkhead box (Fox) protein superfamily that is defined by a conserved winged helix DNA-binding domain1 [16]. FOXM1 is a critical proliferation-associated transcription factor that is widely spatiotemporally expressed during the cell cycle [17]. Centromere protein F (CENPF) is a cell cycle-associated nuclear antigen that is expressed at low levels in G0/G1 cells and accumulates in the nuclear matrix during S phase, with maximal expression in G2/M cells [18]. Kinesin family member 20A (KIF20A), previously named MKLP2 and RAB6KIFL, is located on chromosome 5q31.2 [19]. KIF20A mainly accumulates in the central region of the mitotic cell spindle and participates in cell mitosis [20].

In this study, we revealed that SH3PXD2A-AS1 could promote NSCLC cell proliferation and accelerate cell cycle progression in vitro and in vivo. SH3PXD2A-AS1 interacted with ATP-dependent RNA helicase A (DHX9) to promote the expression of FOXM1 and further led to NSCLC cell proliferation and cell cycle progression.

Methods

Bioinformatics analysis

GEPIA [21] (http://gepia.cancer-pku.cn/detail.php) was used to analyse the expression of SH3PXD2A-AS1 in NSCLC and normal lung tissues and in lung adenocarcinoma (LUAD) and normal lung tissues in TCGA database. In addition, K-M analysis was performed to explore the effects of target genes on the survival

rate in NSCLC and LUAD. Correlation analysis showed the correlation between the genes using the nonlog scale for calculation and the log-scale axis for visualization.

Clinical samples

NSCLC tissues were obtained from the Affiliated Hospital of Xuzhou Medical University. All specimens were pathologically confirmed as NSCLC, and the patients had not received radiotherapy or chemotherapy prior to surgery at the Affiliated Hospital of Xuzhou Medical University. After resection, the tumour and adjacent tissues were frozen in liquid nitrogen, and the specimens were immediately stored at −80°C. The patient studies were conducted in accordance with the Declaration of Helsinki. This study was conducted in compliance with the Declaration of Helsinki. The use of these specimens and data for research purposes was approved by the Ethics Committee of the Affiliated Hospital of Xuzhou Medical University.

Cell lines and cell culture

The immortalized normal human lung epithelial cell line BEAS-2B and the human NSCLC cell lines A549, H1299, H292 and H23 were purchased from the Shanghai Institute of Biochemistry and Cell Biology, Chinese Academy of Science (Shanghai China). BEAS-2B, A549, H1299, H292 and H23 cells were cultured in DMEM medium and RPMI 1640 medium supplemented with 10% foetal bovine serum, 100 U/ml penicillin, and 100 μg/ml streptomycin and incubated in a 37°C humidified incubator with 5% CO_2.

Transient transfections and stable cell lines

PCDNA3.1-SH3PXD2A-AS1, PCDNA3.1-vector, shRNA-SH3PXD2A-AS1, and shRNA-ctrl vectors were transfected into NSCLC cells by Lipofectamine 2000 transfection reagent (Invitrogen, Shanghai, China). SiRNA-DHX9 was transfected into NSCLC cells by SilenFect reagent (Thermo Fisher Scientific, Inc., USA), while nonspecific siRNA was used as a negative control. All siRNAs were purchased from GenePharma Technology (Shanghai, China). SH3PXD2A-AS1 shRNA sequences were cloned into the vector pLko.1 at Age1/ECOR1 sites. SH3PXD2A-AS1 knockdown lentiviruses were generated by cotransfecting 293T cells with two packaging vectors, pMD2G and psPAX. The supernatants of cultured 293T cells were collected 48 h later, filtered through 0.45-mm filters (Millipore, Temecula, CA, USA) and concentrated using Amico Ultra centrifugal filters (Millipore 100 KD MWCO). H292 cells were infected with lentivirus for 48 h and then selected with 2 ng/ml puromycin for 2 weeks, with the medium refreshed every 3 days. The sequences are listed in below:

shSH3PXD2A-AS1#1-For:
CCGGGCAGCTCAGGTGTATGTAAGGCTCGAGCCTTACATACACCTGAGCTGCTTTTTG;

shSH3PXD2A-AS1#1-Rev:
AATTCAAAAAGCAGCTCAGGTGTATGTAAGGCTCGAGCCTTACATACACCTGAGCTGC;

shSH3PXD2A-AS1#2-For:
CCGGGCACCAAGAGAGCCCTAAAGACTCGAGTCTTTAGGGCTCTCTTGGTGCTTTTTG;

shSH3PXD2A-AS1#2-Rev:
AATTCAAAAAGCACCAAGAGAGCCCTAAAGACTCGAGTCTTTAGGGCTCTCTTGGTGC.

siDHX9#1: GAGCCAACUUGAAGGAUUATTUAAUCCUUCAAGUUGGCUCTT

siDHX9#2: CCUGGGAUGAUGCUAGAAUTTAUUCUAGCAUCAUCCCAGGTT

Cell proliferation and colony formation assays

Forty-eight hours after transfection, for CCK-8 analysis, ~4 × 10^3 cells were seeded in each well of 96-well plates, and CCK-8 solution was added 24, 48, 72, and 96 h after placing. Cells were incubated at 37°C for 2 h after 10 μl of CCK-8 solution was added. The absorbance at 450 nm was measured. For the colony formation assay, 1 × 10^3 cells were cultured in six-well plates at 37°C for 14 days; visible colonies were washed twice with PBS, fixed, and stained with 4% paraformaldehyde and crystal violet. The area of colony formation is measured by Image Pro Plus 6.0 and calculated with graphpad.

Cell cycle analysis

Cells were treated with 1 μg/ml aphidicolin at 48 hours after transfection. After 12 h, the cells were incubated in fresh medium containing 50 ng/ml nocodazole for 0, 3 or 6 h. Then, the cells were fixed with 70% cold ethanol at 4°C overnight and stained with 40 μg/ml propidium iodide in hypotonic fluorochrome buffer for 30 min. The samples were then analysed using a FACSCanto flow cytometer (BD Biosciences, San Jose, CA).

RNA extraction, reverse transcription-PCR and qRT-PCR

Total RNA from the lung tissue specimens and cell lines used in this study was extracted with TRIzol reagent (Vazyme Biotech, Nanjing, China). We synthesized cDNA by using HiScript Q RT SuperMix for qPCR (+gDNA wiper) (Vazyme Biotech, Nanjing, China). Relative RNA levels determined by RT-qPCR were measured on a Roche LightCycler 480 by using UltraSYBR Mixture (CWBIO, Beijing, China). The primers used for quantitative RT-PCR analysis are listed below:

SH3PXD2A-AS1-For: CAGGAGTGTGCCACCATGCTTG;

SH3PXD2A-AS1-Rev: GGCAAGACTGGCTCATGAACTCTC;

SERPINB3-For: AGATTAACTCCTGGGTGGAAAG;

SERPINB3-Rev: CAATGTGGTATTGCTGCCAATA;

KIF20A-For: GAATGTGGAGACCCTTGTTCTA;

KIF20A-Rev: CCATCTCCTTCACAGTTAGGTT;

CENPF-For: TACAACGAGAGAGTAAGAACGC;

CENPF-Rev: CTACCTCCACTGACTTACTGTC;

FOXM1-For: GATCTGCGAGATTTTGGTACAC;

FOXM1-Rev: CTGCAGAAGAAAGAGGAGCTAT;

IFNB-1-For: TGGCTGGAATGAGACTATTGTT;

IFNB-1-Rev: GGTAATGCAGAATCCTCCCATA;

LGALS3-For: CAGACAATTTTTCGCTCCATGA;

LGALS3-Rev: TAGGCCCCAGGATAGGAAG;

TXNIP-For: GTTCAGAAGATCAGGCCTTCTA;

TXNIP-Rev: TCCAGGAACGCTAACATAGATC;

SAMD9-For: GCTTGAAAGTATCCATCGGTTC;

SAMD9-Rev: TCAACTGAAATGTTCCCGTTTC;

DHX9-For: TCCAACTGGAATCCTTGGAC;

DHX9-Rev: TTTTCCCACATCCAGTAGCC;

18S rRNA-For: GTAACCCGTTGAACCCCATT;

18S rRNA-Rev: CCATCCAATCGGTAGTAGCG.

Differential expression analysis and functional enrichment

For identification of differentially expressed genes (DEG) between two different samples, the expression level of each transcript was calculated according to the fragments per kilobase of exon per million mapped reads (FRKM) method. RSEM (http://deweylab.biostat.wisc.edu/rsem/) [22] was used to quantify gene abundances. The R statistical package software EdgeR (Empirical analysis of Digital Gene Expression in R, (http://www.bioconductor.org/packages/2.12/bioc/html/edgeR.html)) [23] was utilized for differential expression analysis. In addition, functional enrichment analysis, including GO and KEGG analyses, was performed to identify which DEGs were significantly enriched in GO terms and metabolic pathways with a Bonferroni-corrected P-value $\leq$0.05 compared with the whole-transcriptome background. GO functional enrichment and KEGG pathway analysis were carried out by Goatools (https://github.com/tanghaibao/Goatools) and KOBAS (http://kobas.cbi.pku.edu.cn/home.do) [24].

Western blotting analysis

Western blotting was carried out as previously reported. Briefly, protein extracts from cells or immunoprecipitation samples were prepared using detergent-containing lysis buffer. Total protein was subjected to SDS-PAGE and transferred to 0.45 μm PVDF membranes (Millipore). Antibodies against FOXM1 (Proteintech, 13147-1-AP, 1:1000, USA), CENPF (Affinity, DF2310, 1:1000, China), KIF20A (Affinity, DF8671, 1:2000 China), Cyclin B1 (Cell Signaling Technology, 12231, 1:1000, USA), HSPA5 (Proteintech, 115871-AP, 1:2000, USA), HSPA8 (Proteintech, 10654-1-AP, 1:2000, USA), DHX9 (Proteintech, 17721-1-AP, 1:2000, USA), and alpha tubulin (Proteintech, 66031-1-Ig, 1:100000, USA) were used for primary antibody incubation at 4 °C overnight.

RNA pulldown assay and mass spectrometry

RNA pulldown assays were carried out as described briefly: in vitro biotin-labelled RNAs (SH3PXD2A-AS1, its antisense RNA) were transcribed with Biotin RNA Labeling Mix (Promega Corporation, USA) and T7 RNA polymerase (Thermo Fisher Scientific, USA) treated with RNase inhibitor and purified with a Clean-up kit (Promega Corporation, USA). The biotinylated SH3PXD2A-AS1 probes were dissolved in binding and washing buffer and incubated with streptavidin agarose resin (Thermo Fisher Scientific, USA). Then, H292 cell lysates were incubated with probe-coated streptavidin beads, and the pulled-down proteins were run on SDS-PAGE gels. Then, the gels were stained with Coomassie Blue, and differentially abundant bands were cut out for mass spectrometry (Shanghai Applied Protein Technology Co., Ltd., China).

RNA immunoprecipitation

The RIP experiment was carried out with the EZ-Magna RIP Kit (Millipore) according to the manufacturer's protocol using 5 mg of antibody. H292 cells were lysed in complete RIP lysis buffer, and the cell extract was incubated with protein A/g agarose beads conjugated with antibody DHX9 (17721-1-AP, Proteintech, USA) or control IgG for 2 hours at 4°C. Beads were washed and incubated with Proteinase K to remove proteins. Finally, purified RNA was subjected to quantitative RT-PCR analysis.

Animal experiments

Female BALB/cJGpt-Foxn1^{nu}/Gpt mice (6-8 weeks old) were purchased from Nanjing GemPharmatech Technology Co., Ltd. (Nanjing, China). All animal experiments were approved by the Animal Care and Use Committee of Xuzhou Medical University. Groups of H292-shCtrl and H292-shSH3PXD2A-AS1 cells (5×10^6) were injected subcutaneously into the flanks of mice. Tumour volume (V) was monitored every 2/3 days by measuring the long axis (L) and the short axis (W) of xenograft tumours and calculated with the following formula: $V = (L\times W^2)/2$.

Immunohistochemistry (IHC)

IHC assays were implemented following a standard streptavidin-peroxidase (SP) method as previously reported [25], and heat-induced epitope retrieval (HIER) was performed with retrieval buffer (citrate, pH 6.0) prior to commencing the IHC staining protocol. For primary antibody incubation, anti-FOXM1 (sc-376471, santa cruz, USA) antibody at a 1:100 dilution and anti-Ki67 (ab16667, Abcam, USA) antibodies at a 1:200 dilution were applied. The slide without primary antibody incubation served as a negative control.

Statistical analysis

Statistical analyses were carried out using SPSS 20.0 software (SPSS, Inc., Chicago, IL, USA) and GraphPad Prism 8. The Kaplan–Meier method and log-rank test were used to evaluate the correlation between SH3PXD2A-AS1 expression and NSCLC/LUAD patient survival. The unpaired t test was used to determine the statistical significance of differences between groups. Data are presented as the mean ± SD. $P<0.05$ was considered statistically significant.

Results

SH3PXD2A-AS1 is upregulated in NSCLC tumour tissues

Microarray analysis through GEPIA was used to identify differentially expressed SH3PXD2A-AS1 in LUAD or NSCLC tissues and adjacent tissues. SH3PXD2A-AS1 expression in the LUAD or NSCLC tissues was upregulated compared with that in the normal lung tissues (Fig. 1a). In addition, a prognostic analysis of SH3PXD2A-AS1 was performed, and the results demonstrated that high expression of SH3PXD2A-AS1 had an adverse effect on survival, as shown by Kaplan-Meier analysis (Fig. 1b). Then, we performed qRT-PCR analysis to investigate the SH3PXD2A-AS1 expression level, which was significantly higher in the tumour tissues than in the corresponding normal tissues (Fig. 1c).

SH3PXD2A-AS1 promotes lung cancer cell proliferation and accelerates cell cycle progression in vitro

To explore the biological functions of SH3PXD2A-AS1 in lung cancer cells, we first examined SH3PXD2A-AS1 expression in the immortalized normal human lung epithelial cell line BEAS-2B and a series of lung cancer cell lines, including A549, H1299, H292 and H23, by qRT-PCR (Fig. 2a). SH3PXD2A-AS1 expression in the lung cancer cell lines was higher than that in the normal human lung epithelial cell line and was much higher in H292 and H23 cells than the other cells. Then, a full-length recombinant plasmid with SH3PXD2A-AS1 was used to increase SH3PXD2A-AS1 expression in A549 and H1299 cells (Fig. 2b), whereas lentivirus-mediated control shRNA or an effective SH3PXD2A-AS1 shRNA was used to specifically knock down SH3PXD2A-AS1 expression in H292 and H23 cells (Fig. 2c). SH3PXD2A-AS1 expression was substantially up- or downregulated 24 or 48 h after transfection. CCK-8 and colony formation assays revealed that SH3PXD2A-AS1 overexpression promoted cell growth and proliferation of A549 and H1299 cells, while knockdown of SH3PXD2A-AS1 significantly inhibited the growth and proliferation of H292 and H23 cells (Fig. 2d-2e and 2h-2i). Then, we further determined whether SH3PXD2A-AS1 regulates the cell cycle. Flow cytometric analysis showed that upregulation of

SH3PXD2A-AS1 expression increased the percentage of cells in the S and G2 phases, and downregulation of SH3PXD2A-AS1 expression decreased the percentage of cells in the S and G2 phases (Fig. 2f and 2g).

Identification of cytokine-related genes as probable target genes of SH3PXD2A-AS1 in NSCLC proliferation

To further elucidate the mechanism by which SH3PXD2A-AS1 regulates lung cancer proliferation, we conducted gene expression profiling of SH3PXD2A-AS1 knockdown and vector control H292 cells in triplicate (Fig. 3a and S1a-S1b). GO and KEGG enrichment analysis revealed that many biological functions in 894 downregulated genes related to the cell cycle (Fig. 3b). Additionally, we verified the RNA-seq results by qRT-PCR and showed that the mRNA expression levels of CENPF, KIF20A and FOXM1 were decreased among the 8 top differentially expressed genes induced by SH3PXD2A-AS1 knockdown (Fig. 3c). We used pearson correlation analysis and identified a strong correlation between FOXM1 and CENPF (P<0.001, R=0.72) and FOXM1 and KIF20A (P<0.001, R=0.73) (Fig. S2a and S2b). The FOXM1 transcription factor is recognized as a regulator of cell cycle progression; thus, we also examined Cyclin B1. Western blotting was used to test the protein expression levels of FOXM1, Cyclin B1, KIF20A and CENPF, and the results showed that the protein expression was upregulated by SH3PXD2A-AS1 overexpression and inhibited by SH3PXD2A-AS1 knockdown (Fig. 3d and 3e). Then, qRT-PCR was used to test the mRNA expression levels of FOXM1, Cyclin B1, KIF20A and CENPF, and the results showed that these genes were upregulated by SH3PXD2A-AS1 overexpression and inhibited by SH3PXD2A-AS1 knockdown (Fig. 3f and 3g).

SH3PXD2A-AS1 interacts with the DHX9 protein

LncRNAs have been reported to exert biological functions by interacting with proteins. Therefore, to identify the SH3PXD2A-AS1-binding proteins, we performed in vitro transcription assays and RNA pulldown assays by using biotin-labelled SH3PXD2A-AS1 and a negative control in H292 cells (Fig. 4a). We performed Western blot analysis on RNA pulldown material to verify the MS results. The results indicated that SH3PXD2A-AS1 was associated with DHX9 but not HSPA8 or HSPA5 (Fig. 4b). Moreover, RIP assays were performed to confirm the significant interaction of SH3PXD2A-AS1 with DHX9 in H292 cells (Fig. 4c).

Knockdown of DHX9 inhibits cell proliferation and cell cycle progression

To determine the role of DHX9 in SH3PXD2A-AS1-mediated cell proliferation, we first employed western blotting and PCR to determine the effects of DHX9. The results indicated that knockdown of DHX9 by siRNAs inhibited the expression of FOXM1, Cyclin B1, KIF20A and CENPF at both the protein and mRNA levels in H292 and H23 cells (Fig. 5a and 5b). Then, we observed that the H292 and H23 cells with DHX9 knockdown showed significantly inhibited cell proliferation compared with the control cells (Fig. 5c and 5e). Furthermore, we found that the H292 and H23 cells with DHX9 knockdown had decreased percentages of cells in the S and G2 phases (Fig. 5d).

DHX9 knockdown reverses the effects on proliferation and cell cycle progression induced by SH3PXD2A-AS1 overexpression

To assess the requirement for DHX9 in the inhibition of proliferation and cell cycle progression induced by SH3PXD2A-AS1 overexpression, we silenced DHX9 by siRNA in H1299 and A549 cells with SH3PXD2A-AS1 overexpression (Fig. 6b). First, the Western blotting results showed that the FOXM1, Cyclin B1, KIF20A and CENPF levels, which were upregulated by SH3PXD2A-AS1 overexpression, were subsequently recovered following DHX9 knockdown (Fig. 6a). Moreover, the results showed that the increases in proliferation and the percentage of cells in the S and G2 phases caused by SH3PXD2A-AS1 overexpression were reversed by transient transfection of DHX9 siRNA in H1299 and A549 cells (Fig. 6c-6e). These results demonstrated that DHX9 plays a crucial role in SH3PXD2A-AS1-regulated cell proliferation and cell cycle progression.

Knockdown of SH3PXD2A-AS1 inhibits NSCLC cell proliferation in vivo

To further confirm the role of SH3PXD2A-AS1 in vivo, we used a xenograft mouse model. H292 cells stably transfected with sh-SH3PXD2A-AS1 or an empty vector were subcutaneously injected into nude mice (control on left, sh-SH3PXD2A-AS1 on right). The results showed that the tumours derived from the SH3PXD2A-AS1 stable knockdown cells exhibited significantly smaller tumour volumes (Fig. 7a) and a lower tumour growth capacity (Fig. 7b) than the tumours from the control group. Seventeen days after injection, the average tumour weight in the sh-SH3PXD2A-AS1 group was significantly lower than that in the control group (Fig. 7c). Furthermore, IHC staining of tissue sections showed that the tumour tissues from the SH3PXD2A-AS1 knockdown group had a weaker staining intensity of Ki67 and FOXM1 than those from the control group (Fig. 7e). Taken together, these results suggest that knockdown of SH3PXD2A-AS1 inhibits the proliferation of NSCLC cells in vivo.

Discussion

Lung cancer is the leading cause of cancer-related death. Improved predictive biomarkers are needed so that cancer patients can be provided with the most effective treatments available, as well as a larger repertoire of therapeutic targets. Emerging studies have shown that lncRNAs play a critical role in cancer. Although many lncRNAs have been identified in the human genome, very few have been experimentally validated and functionally annotated in lung cancer [26–28]. In the present study, we investigated a novel lncRNA (SH3PXD2A-AS1) that is markedly upregulated in lung cancer tissues. SH3PXD2A-AS1 is an antisense transcript transcribed from SH3PXD2A and located on chromosome 10. The SH3PXD2A gene was expressed at higher levels in breast, colon, lung and prostate cancer tissues than in normal tissues [29]. The dysregulation of SH3PXD2A gene expression has been shown in many diverse cancers [30–33], and lncRNA generation in the SH3PXD2A genes may play important roles in tumorigenesis. We showed that increased SH3PXD2A-AS1 expression was associated with a poor prognosis and shorter survival time in NSCLC patients. Our gene expression and functional data strongly support the potential utility of SH3PXD2A-AS1 as a biomarker and as a therapeutic target for NSCLC.

The tumorigenesis and progression of NSCLC is accompanied or driven by infinite proliferation [34, 35]. In our study, we designed a series of experiments to explore the roles of SH3PXD2A-AS1 in NSCLC. Our data showed that SH3PXD2A-AS1 was highly expressed in lung cancer cells compared with normal lung epithelial cells (Fig. 2a). The knockdown of SH3PXD2A-AS1 inhibited lung cancer cell proliferation and colony formation in vitro (Fig. 2e and 2i). Moreover, the knockdown of SH3PXD2A-AS1 had a significant effect on cell cycle progression (Fig. 2g). Together, these results showed that SH3PXD2A-AS1 is an important regulator of lung cancer proliferation.

With regard to the potential of SH3PXD2A-AS1 in lung cancer proliferation, we further investigated the molecular mechanism of its functional properties. In this study, gene expression profiling analysis was used to reveal that hundreds of genes were regulated by SH3PXD2A-AS1 knockdown. We performed GO and KEGG enrichment analysis of 894 downregulated genes, and the results showed many biological functions such as regulation of cell cycle phase transition related to the cell cycle (Fig. 3b). Subsequently, we verified the sequencing results by PCR. Among the 8 top differentially expressed genes, SH3PXD2A-AS1 was selected, and knockdown of this gene suppressed the expression of FOXM1, CENPF and KIF20A (Fig. 3c). There were strong correlations between FOXM1 and CENPF and between FOXM1 and KIF20A (Fig. S2a and S2b). FOXM1 has an effect on the biological functions of various cancers through synergistic interactions or transcriptional regulation with CENPF [36–38] and KIF20A [39–41]. Because FOXM1 has a strong correlation and synergistic interaction or transcriptional regulation with CENPF and KIF20A, we selected FOXM1 as the main gene for the following experiment. FOXM1 is a critical proliferation-associated transcription factor that is widely spatiotemporally expressed during the cell cycle [42, 43]. FOXM1 is essential for progression to DNA replication and mitosis and stimulates the proliferation of tumour cells during the progression of NSCLC via the Cyclin A2 and Cyclin B1 genes [44]. In our study, we found that FOXM1, Cyclin B1, KIF20A and CENPF were inhibited by SH3PXD2A-AS1 knockdown (Fig. 3e). These findings indicated that FOXM1, CENPF and KIF20A contributed to SH3PXD2A-AS1-regulated lung cancer cell proliferation.

Given that cytokine changes resulted from SH3PXD2A-AS1 knockdown, we then elucidated the signalling pathways by which SH3PXD2A-AS1 regulated these cytokines. Generally, lncRNAs exert their function by interacting with various RNA binding proteins (RBPs), leading to inactivation or activation of gene expression. Therefore, we used biotin-labelled SH3PXD2A-AS1 in RNA pulldown assays to obtain interacting partners for mass spectrometry. The results indicated that DHX9 might be the most important common transcriptional regulator (Fig. 4a and b). Moreover, RIP assays confirmed that SH3PXD2A-AS1 could bind to DHX9 in H292 cells (Fig. 4c). DHX9 is a member of the DExD/H-box family of helicases and appears to play a central role in many cellular processes, with the ability to unwind DNA and RNA duplexes [45]. In cervical cancer cells, the proto-oncogene DHX9 binds to LNCRNA and MDM2 to regulate cell invasion and angiogenesis [46]. Our present data suggest that knockdown of DHX9 distinctly inhibits cell proliferation and cell cycle progression. In addition, downregulation of DHX9 leads to the depletion of FOXM1, Cyclin B1, CENPF and KIF20A. To further confirm the interaction between DHX9 and SH3PXD2A-AS1, we silenced DHX9 in NSCLC cells overexpressing SH3PXD2A-AS1. Our data showed that silencing DHX9 suppresses the cell proliferation, cell cycle progression and changes in expression of the

downstream factor FOXM1 induced by overexpression of SH3PXD2A-AS1 (Fig. 6a-6e). Hence, we revealed that SH3PXD2A-AS1 interacts with DHX9 to enhance FOXM1 expression to promote cell proliferation and cell cycle progression.

Conclusion

Our study shows for the first time that aberrant expression of SH3PXD2A-AS1 contributes to the proliferation and cell cycle progression of NSCLC. SH3PXD2A-AS1 regulates the expression of FOXM1 by binding to DHX9 in lung cancer cells to promote cell proliferation and cell cycle progression. These findings identify SH3PXD2A-AS1 as a potential biomarker and target for prognosis and therapy of NSCLC.

Abbreviations

lncRNA: long noncoding RNAs; NSCLC: non–small cell lung carcinoma; TCGA: The Cancer Genome Atlas; LUAD: lung adenocarcinoma; FOXM1: Forkhead box protein M1; KIF20A: kinesin family member 20A; CENPF: centromere protein F; DHX9: ATP-dependent RNA helicase A; RIP: RNA immunoprecipitation; IHC: immunohistochemistry.

Declarations

Acknowledgments

We thank the National Natural Science Foundation of China, Natural Science Foundation of Jiangsu Province, and Xuzhou Municipal Science and Technology Bureau for their financial support. We thank all members of Thoracic Surgery Laboratory and Cancer Institute of Xuzhou Medical University for useful discussions.

Authors' contributions

YQZ, HZ, and JB conceived the project. YQZ, HMY, SFC, MLL, and ZWL performed the experiments. All authors contributed to experimental design and data analysis. YQZ, and HMY composed the manuscript. HZ and JB verified the underlying data. All authors contributed to the writing and approved the final version of this manuscript.

Funding

Funding was provided by the Social Development Projects of Key R&D Programs in Jiangsu Province (BE2019643), the National Natural Science Foundation of Jiangsu Province (BK20171178), the General

Program of Jiangsu Commission of Health (H2017083), the Project of Invigorating Health Care through Science, Technology and Education, the Jiangsu Provincial Medical Youth Talent (QNRC2016778), and the Foundation of Jiangsu Province Six Talents Peak (2015-WSN-063).

Availability of data and materials

The datasets used and/or analyzed during the current study are available from the corresponding author on reasonable request.

Ethics approval and consent to participate

This study was conducted in compliance with the declaration of Helsinki. Informed consent was obtained from all subjects. The ethics approval statements for human subjects were provided by the Ethnic Committee of the Affiliated Hospital of Xuzhou Medical University. The ethics approval statements for animal work were provided by the Institutional Animal Care and Use Committee of Xuzhou Medical University.

Consent for publication

Not applicable.

Author details

[1]Thoracic Surgery Laboratory, The First College of Clinical Medicine, Xuzhou Medical University, Xuzhou 221006, Jiangsu Province, China. [2]Department of Thoracic Surgery, Affiliated Hospital of Xuzhou Medical University, 99 West Huaihai Road, Xuzhou 221006, Jiangsu, China.

Competing Interest

The authors declare that they have no competing interests.

References

1. Siegel RL, Miller KD, Jemal A. Cancer statistics. 2019. CA Cancer J Clin. 2019; 69(1): 7–34.

2. Hirsch FR, Scagliotti GV, Mulshine JL, Kwon R, Curran WJ Jr, Wu YL, et al. Lung cancer: current therapies and new targeted treatments. Lancet. 2017;389(10066):299–311.
3. Wang X, Adjei AA. Lung cancer and metastasis: new opportunities and challenges. Cancer Metastasis Rev. 2015;34(2):169–71.
4. Huarte M. The emerging role of lncRNAs in cancer. Nat Med. 2015;21(11):1253–61.
5. Statello L, Guo CJ, Chen LL, Huarte M. Gene regulation by long non-coding RNAs and its biological functions. Nat Rev Mol Cell Biol. 2020.
6. Kim J, Piao HL, Kim BJ, Yao F, Han Z, Wang Y, et al. Long noncoding RNA MALAT1 suppresses breast cancer metastasis. Nat Genet. 2018;50(12):1705–15.
7. Yang B, Zhang L, Cao Y, Chen S, Cao J, Wu D, et al. Overexpression of lncRNA IGFBP4-1 reprograms energy metabolism to promote lung cancer progression. Mol Cancer. 2017;16(1):154.
8. Pan J, Fang S, Tian H, Zhou C, Zhao X, Tian H, et al. lncRNA JPX/miR-33a-5p/Twist1 axis regulates tumorigenesis and metastasis of lung cancer by activating Wnt/beta-catenin signaling. Mol Cancer. 2020;19(1):9.
9. Zhuo W, Liu Y, Li S, Guo D, Sun Q, Jin J, et al. Long Noncoding RNA GMAN, Up-regulated in Gastric Cancer Tissues, Is Associated With Metastasis in Patients and Promotes Translation of Ephrin A1 by Competitively Binding GMAN-AS. Gastroenterology. 2019;156(3):676–91. e611.
10. Li C, Zhao W, Pan X, Li X, Yan F, Liu S, et al. LncRNA KTN1-AS1 promotes the progression of non-small cell lung cancer via sponging of miR-130a-5p and activation of PDPK1. Oncogene. 2020;39(39):6157–71.
11. Sun L, Wang L, Chen T, Shi Y, Yao B, Liu Z, et al. LncRNA RUNX1-IT1 which is downregulated by hypoxia-driven histone deacetylase 3 represses proliferation and cancer stem-like properties in hepatocellular carcinoma cells. Cell Death Dis. 2020;11(2):95.
12. Zhang E, He X, Zhang C, Su J, Lu X, Si X, et al. A novel long noncoding RNA HOXC-AS3 mediates tumorigenesis of gastric cancer by binding to YBX1. Genome Biol. 2018;19(1):154.
13. Yang X, Song JH, Cheng Y, Wu W, Bhagat T, Yu Y, et al. Long non-coding RNA HNF1A-AS1 regulates proliferation and migration in oesophageal adenocarcinoma cells. Gut. 2014;63(6):881–90.
14. Ma Z, Peng P, Zhou J, Hui B, Ji H, Wang J, et al. Long Non-Coding RNA SH3PXD2A-AS1 Promotes Cell Progression Partly Through Epigenetic Silencing P57 and KLF2 in Colorectal Cancer. Cellular physiology and biochemistry: international journal of experimental cellular physiology, biochemistry, and pharmacology. 2018; 46(6): 2197–2214.
15. Guo S, Zhu KX, Yu WH, Wang T, Li S, Wang YX, et al. SH3PXD2A-AS1/miR-330-5p/UBA2 ceRNA network mediates the progression of colorectal cancer through regulating the activity of the Wnt/beta-catenin signaling pathway. Environ Toxicol. 2020.
16. Clark KL, Halay ED, Lai E, Burley SK. Co-crystal structure of the HNF-3/fork head DNA-recognition motif resembles histone H5. Nature. 1993;364(6436):412–20.

17. Liao GB, Li XZ, Zeng S, Liu C, Yang SM, Yang L, et al. Regulation of the master regulator FOXM1 in cancer. Cell Commun Signal. 2018;16(1):57.
18. Sun J, Huang J, Lan J, Zhou K, Gao Y, Song Z, et al. Overexpression of CENPF correlates with poor prognosis and tumor bone metastasis in breast cancer. Cancer Cell Int. 2019;19:264.
19. Echard A, Jollivet F, Martinez O, Lacapere JJ, Rousselet A, Janoueix-Lerosey I, et al. Interaction of a Golgi-associated kinesin-like protein with Rab6. Science. 1998;279(5350):580–5.
20. Lai F, Godley LA, Joslin J, Fernald AA, Liu J, Espinosa R 3. Transcript map and comparative analysis of the 1.5-Mb commonly deleted segment of human 5q31 in malignant myeloid diseases with a del(5q). Genomics. 2001;71(2):235–45. rd et al.
21. Tang Z, Li C, Kang B, Gao G, Li C, Zhang Z. GEPIA: a web server for cancer and normal gene expression profiling and interactive analyses. Nucleic acids research. 2017;45(W1):W98–102.
22. Li B, Dewey CN. RSEM: accurate transcript quantification from RNA-Seq data with or without a reference genome. BMC Bioinformatics. 2011;12:323.
23. Robinson MD, McCarthy DJ, Smyth GK. edgeR: a Bioconductor package for differential expression analysis of digital gene expression data. BIOINFORMATICS. 2010;26(1):139–40.
24. Xie C, Mao X, Huang J, Ding Y, Wu J, Dong S, et al. KOBAS 2.0: a web server for annotation and identification of enriched pathways and diseases. Nucleic Acids Res. 2011;39:W316–22. (Web Server issue).
25. Hou PF, Jiang T, Chen F, Shi PC, Li HQ, Bai J, et al. KIF4A facilitates cell proliferation via induction of p21-mediated cell cycle progression and promotes metastasis in colorectal cancer. Cell death disease. 2018;9(5):477.
26. Yang J, Qiu Q, Qian X, Yi J, Jiao Y, Yu M, et al. Long noncoding RNA LCAT1 functions as a ceRNA to regulate RAC1 function by sponging miR-4715-5p in lung cancer. Mol Cancer. 2019;18(1):171.
27. Hua Q, Jin M, Mi B, Xu F, Li T, Zhao L, et al. LINC01123, a c-Myc-activated long non-coding RNA, promotes proliferation and aerobic glycolysis of non-small cell lung cancer through miR-199a-5p/c-Myc axis. J Hematol Oncol. 2019;12(1):91.
28. Chen Z, Li JL, Lin S, Cao C, Gimbrone NT, Yang R, et al. cAMP/CREB-regulated LINC00473 marks LKB1-inactivated lung cancer and mediates tumor growth. J Clin Invest. 2016;126(6):2267–79.
29. Stylli SS, Luwor RB, Kaye AH, I ST, Hovens CM, Lock P. Expression of the adaptor protein Tks5 in human cancer: prognostic potential. Oncol Rep. 2014;32(3):989–1002.
30. Iizuka S, Abdullah C, Buschman MD, Diaz B, Courtneidge SA. The role of Tks adaptor proteins in invadopodia formation, growth and metastasis of melanoma. Oncotarget. 2016;7(48):78473–86.
31. Stylli SS, I ST, Kaye AH, Lock P. Prognostic significance of Tks5 expression in gliomas. J Clin Neurosci. 2012;19(3):436–42.
32. Daly C, Logan B, Breeyear J, Whitaker K, Ahmed M, Seals DF. Tks5 SH3 domains exhibit differential effects on invadopodia development. PLoS One. 2020;15(1):e0227855.

33. Seals DF, Azucena EF Jr, Pass I, Tesfay L, Gordon R, Woodrow M, et al. The adaptor protein Tks5/Fish is required for podosome formation and function, and for the protease-driven invasion of cancer cells. Cancer Cell. 2005;7(2):155–65.
34. Yin D, Lu X, Su J, He X, De W, Yang J, et al. Long noncoding RNA AFAP1-AS1 predicts a poor prognosis and regulates non-small cell lung cancer cell proliferation by epigenetically repressing p21 expression. Mol Cancer. 2018;17(1):92.
35. Sun Y, Jin SD, Zhu Q, Han L, Feng J, Lu XY, et al. Long non-coding RNA LUCAT1 is associated with poor prognosis in human non-small lung cancer and regulates cell proliferation via epigenetically repressing p21 and p57 expression. Oncotarget. 2017;8(17):28297–311.
36. Lin SC, Kao CY, Lee HJ, Creighton CJ, Ittmann MM, Tsai SJ, et al. Dysregulation of miRNAs-COUP-TFII-FOXM1-CENPF axis contributes to the metastasis of prostate cancer. Nat Commun. 2016;7:11418.
37. Lokody I. Signalling. FOXM1 and CENPF: co-pilots driving prostate cancer. Nat Rev Cancer. 2014;14(7):450–1.
38. Aytes A, Mitrofanova A, Lefebvre C, Alvarez MJ, Castillo-Martin M, Zheng T, et al. Cross-species regulatory network analysis identifies a synergistic interaction between FOXM1 and CENPF that drives prostate cancer malignancy. Cancer Cell. 2014;25(5):638–51.
39. Xiu G, Sui X, Wang Y, Zhang Z. FOXM1 regulates radiosensitivity of lung cancer cell partly by upregulating KIF20A. Eur J Pharmacol. 2018;833:79–85.
40. Li Y, Guo H, Wang Z, Bu H, Wang S, Wang H, et al. Cyclin F and KIF20A, FOXM1 target genes, increase proliferation and invasion of ovarian cancer cells. Exp Cell Res. 2020;395(2):112212.
41. Khongkow P, Gomes AR, Gong C, Man EP, Tsang JW, Zhao F, et al. Paclitaxel targets FOXM1 to regulate KIF20A in mitotic catastrophe and breast cancer paclitaxel resistance. Oncogene. 2016;35(8):990–1002.
42. Kelleher FC, O'Sullivan H. FOXM1 in sarcoma: role in cell cycle, pluripotency genes and stem cell pathways. Oncotarget. 2016;7(27):42792–804.
43. Hu G, Yan Z, Zhang C, Cheng M, Yan Y, Wang Y, et al. FOXM1 promotes hepatocellular carcinoma progression by regulating KIF4A expression. J Exp Clin Cancer Res. 2019;38(1):188.
44. Kim IM, Ackerson T, Ramakrishna S, Tretiakova M, Wang IC, Kalin TV, et al. The Forkhead Box m1 transcription factor stimulates the proliferation of tumor cells during development of lung cancer. Cancer Res. 2006;66(4):2153–61.
45. Lee T, Pelletier J. The biology of DHX9 and its potential as a therapeutic target. Oncotarget. 2016;7(27):42716–39.
46. Ding X, Jia X, Wang C, Xu J, Gao SJ, Lu C. A DHX9-lncRNA-MDM2 interaction regulates cell invasion and angiogenesis of cervical cancer. Cell Death Differ. 2019;26(9):1750–65.

Figures

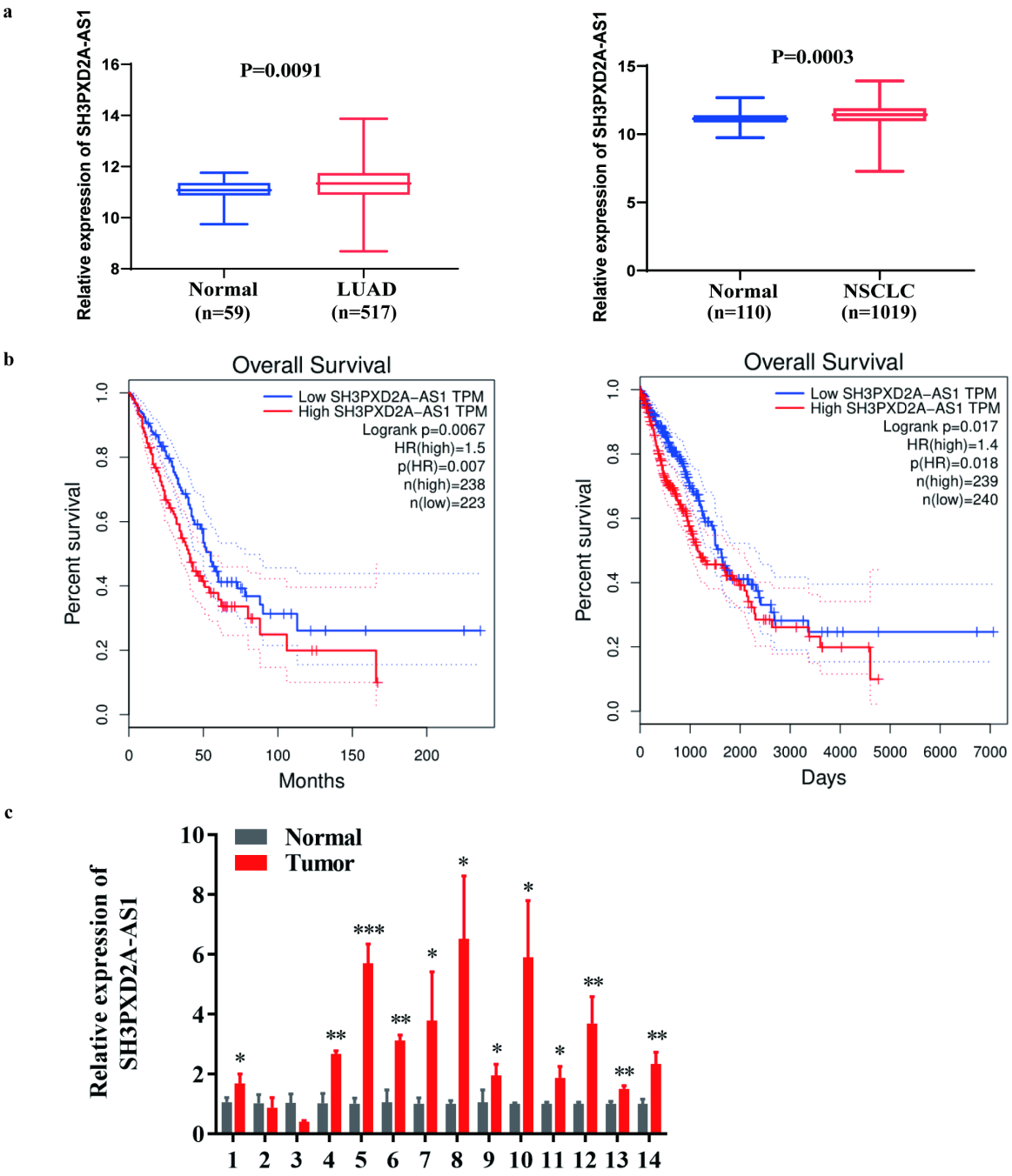

Figure 1

SH3PXD2A-AS1 is upregulated in NSCLC tumour tissues. (a) SH3PXD2A-AS1 expression was analysed in LUAD (n=517, P<0.01) or NSCLC tissues (n=1019, P<0.001) and their adjacent noncancerous tissues (n=59, 110) in the GEPIA database. (b) Kaplan–Meier survival curve analysis was performed to explore the effects of the genes on the survival rate in LUAD (P<0.01) and NSCLC (P<0.05). (c) SH3PXD2A-AS1 expression was validated in 14 pairs of NSCLC patient samples by qRT-PCR; N, normal tissue; T, tumour. Data are shown as the mean ± standard deviation from three independent experiments. *P < 0.05, **P < 0.01, ***P < 0.001. Statistical analysis: Data were performed using unpaired t test (a, c), Kaplan–Meier method and log-rank test (b).

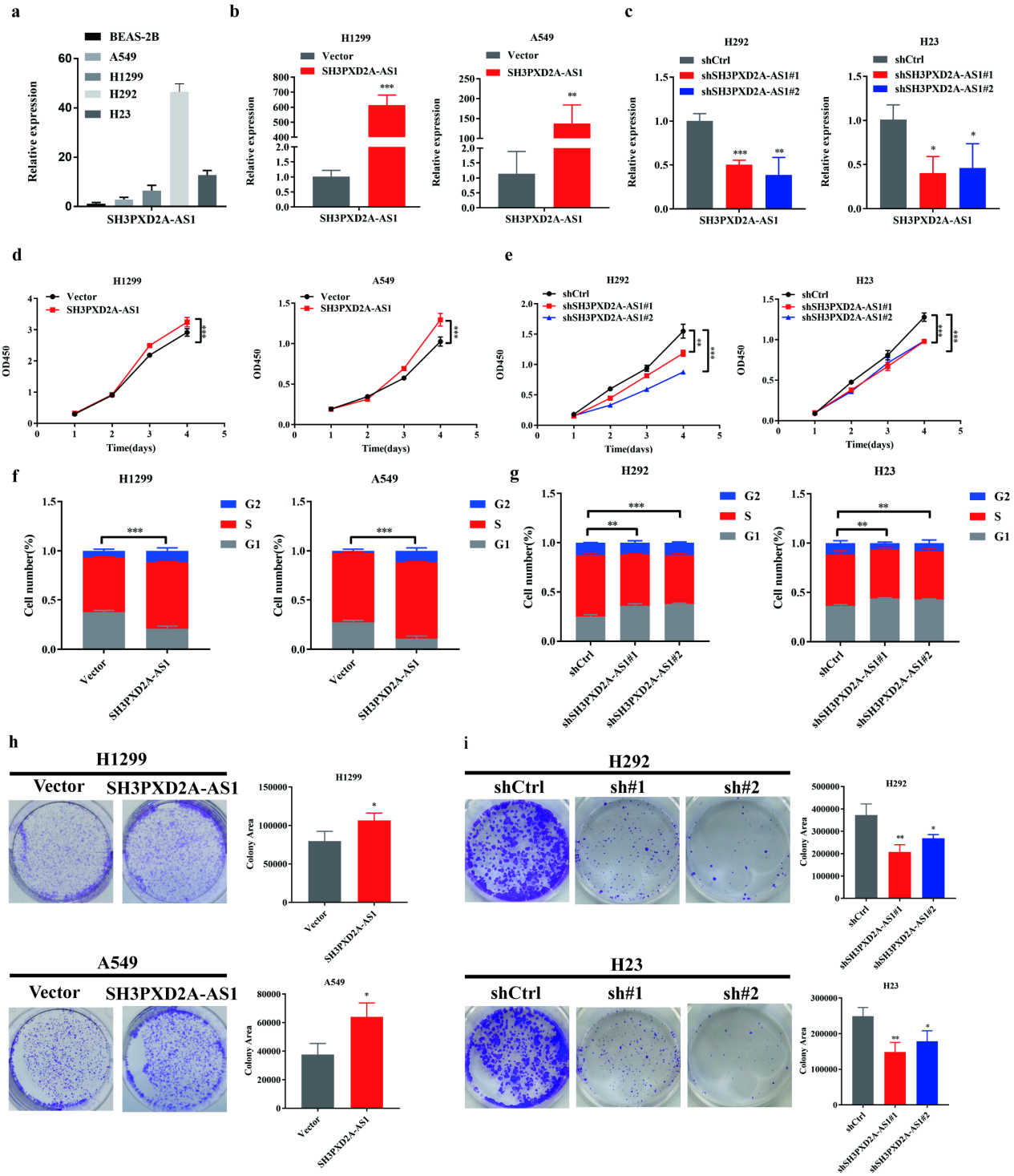

Figure 2

SH3PXD2A-AS1 promoted lung cancer cell proliferation and accelerated cell cycle progression in vitro. (a) The expression level of SH3PXD2A-AS1 was detected by qRT-PCR in four NSCLC cell lines (A549, H1299, H292, and H23) and an immortalized normal human lung epithelial cell line (BEAS-2B). (b) Overexpression of SH3PXD2A-AS1 was confirmed at the mRNA level in A549 and H1299 cells by qRT-PCR. (c) Knockdown of SH3PXD2A-AS1 was confirmed at the mRNA level in H292 and H23 cells by qRT-

PCR. (d, e) Effect of SH3PXD2A-AS1 KD or OE on A549, H1299, H292 and H23 cell proliferation as assessed by Cell Counting Kit-8 (CCK-8) assays. (f, g) The percentage of S/G2 population cells was measured by flow cytometry for SH3PXD2A-AS1 KD or OE A549, H1299, H292 and H23 cell lines. (h, i) Colony formation assays for SH3PXD2A-AS1 KD or OE A549, H1299, H292 and H23 cell lines. Data are shown as the mean ± standard deviation from three independent experiments. *P < 0.05, **P < 0.01, ***P < 0.001. Statistical analysis: Data were performed using unpaired t test (b-i).

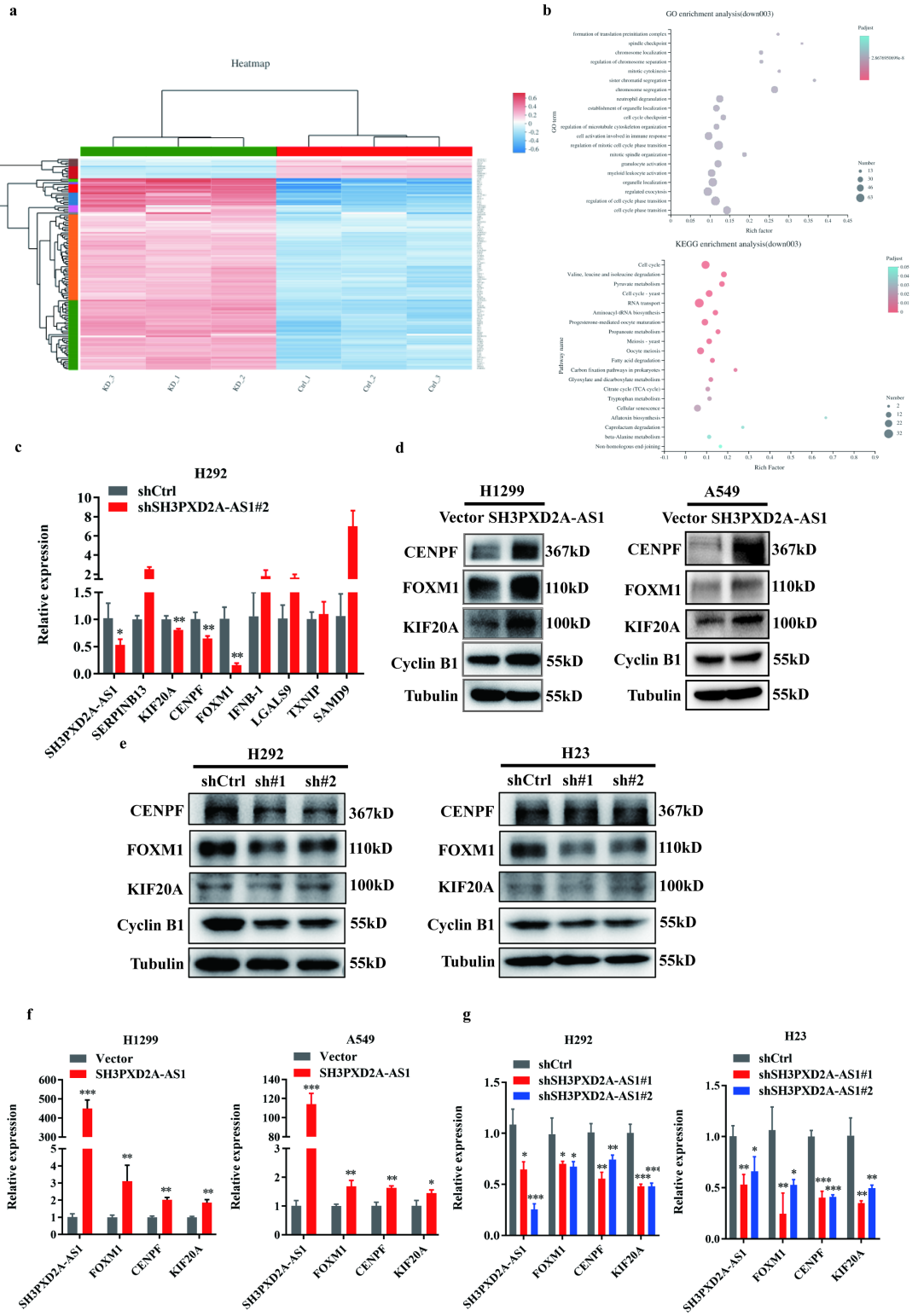

Figure 3

Identification of cytokine-related genes as probable target genes of SH3PXD2A-AS1 in NSCLC proliferation. (a) Cluster analysis of expression patterns of genes/transcripts in the selected gene set. The colour in the figure represents the normalized expression value of the gene in each sample. Red represents higher expression of the gene in the sample, and blue represents lower expression. (b) GO and KEGG enrichment analyses were used to classify the significantly differentially expressed genes of cancer cells. (c) The significantly differentially expressed genes of H292 cells with SH3PXD2A-AS1 knockdown in sequencing results were verified by qRT-PCR. (d, e) Effect of SH3PXD2A-AS1 KD or OE on the expression of the FOXM1, KIF20A and CENPF protein levels in A549, H1299, H292 and H23 cells, as assessed by Western blots. Tubulin was used as a reference control. (f, g) Relative mRNA expression levels of SH3PXD2A-AS1, FOXM1, KIF20A and CENPF in A549, H1299, H292 and H23 cells ± SH3PXD2A-AS1 KD/OE. The 18S gene was used as a reference control. Data are shown as the mean ± standard deviation from three independent experiments. *P < 0.05, **P < 0.01, ***P < 0.001. Statistical analysis: Data were performed using unpaired t test (c, f-g).

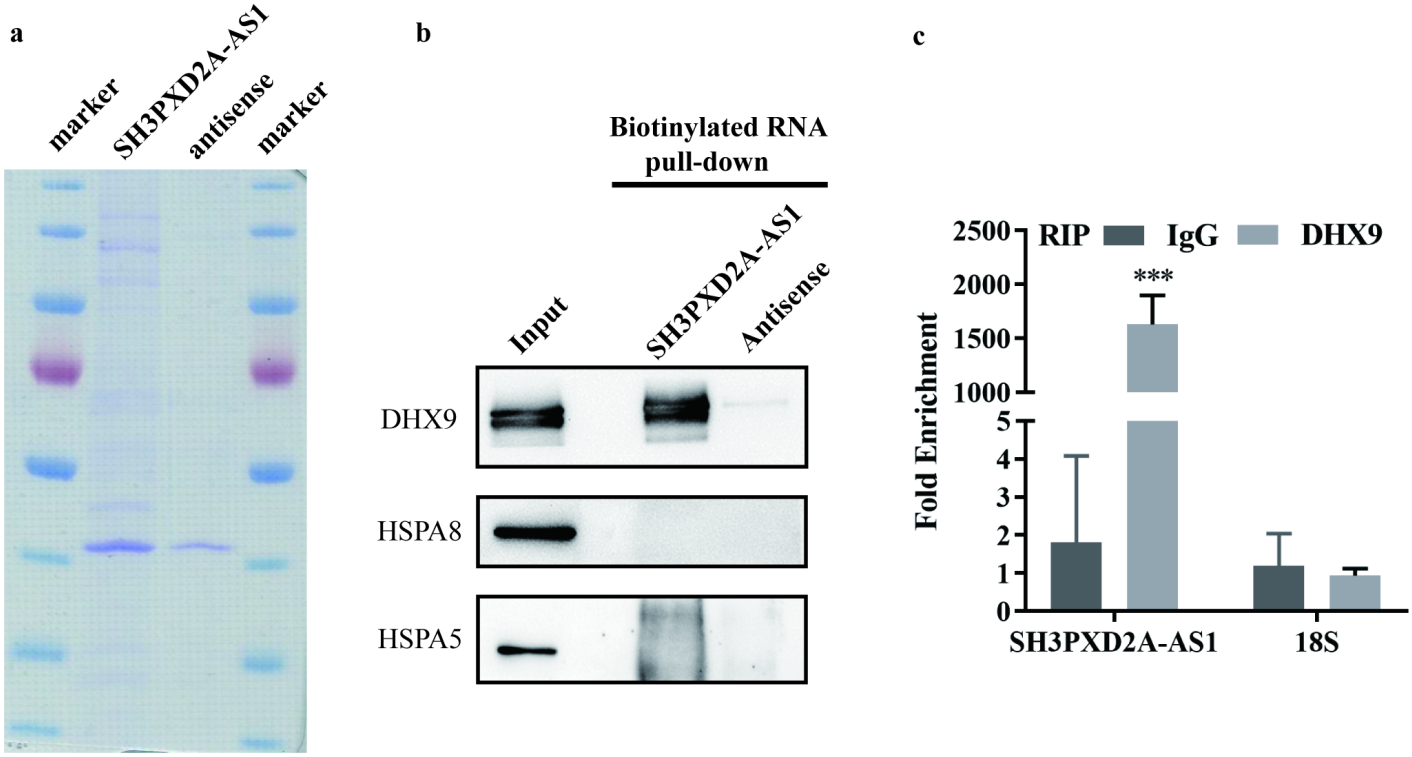

Figure 4

SH3PXD2A-AS1 interacts with the DHX9 protein. (a) Coomassie blue staining of biotinylated SH3PXD2A-AS1-associated proteins is shown. (b) RNA pulldown assays were performed to verify the mass spectrometry results. Biotin-SH3PXD2A-AS1 and antisense RNA were obtained by in vitro transcription by using T7 RNA polymerase. Western blots were used to test DHX9, HSPA8 and HSPA5. (c) RNA immunoprecipitation (RIP) assays were performed to test the interaction of SH3PXD2A-AS1 and DHX9. Relative quantification of SH3PXD2A-AS1 and 18S rRNA in RNA-protein complexes immunoprecipitated with IgG or DHX9 from whole cell extracts; 18S rRNA was used as a negative control binding RNA. Data

are shown as the mean ± standard deviation from three independent experiments. ***P < 0.001. Statistical analysis: Data were performed using unpaired t test (b).

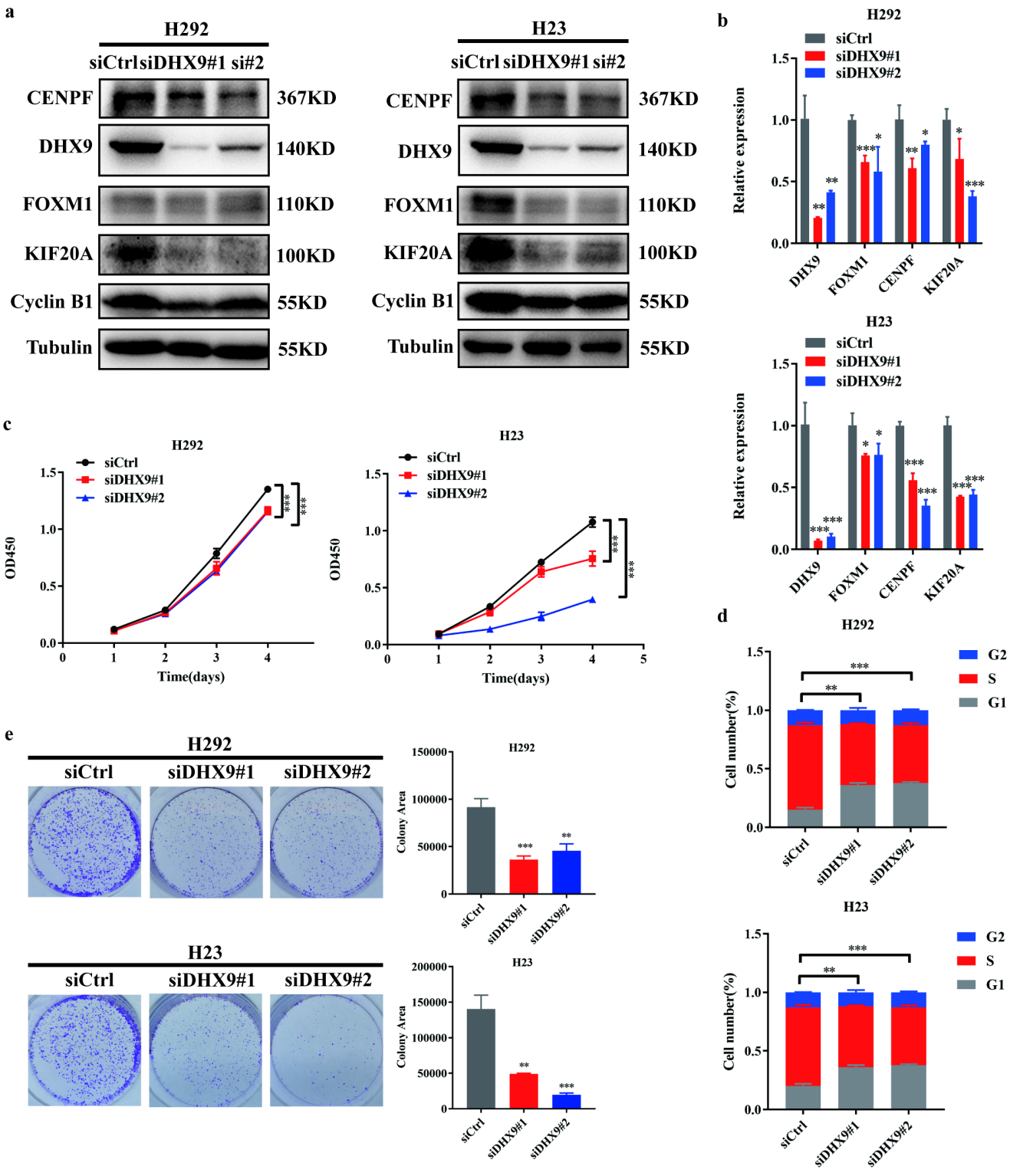

Figure 5

Knockdown of DHX9 inhibits cell proliferation and cell cycle progression. (a) Effect of DHX9 KD on the protein expression of DHX9, FOXM1, Cyclin B1, KIF20A and CENPF in H292 and H23 cells, as assessed by Western blots. (b) Effect of DHX9 KD on the mRNA expression of DHX9, FOXM1, KIF20A and CENPF in

H292 and H23 cells, as assessed by qRT-PCR. (c) Effect of DHX9 KD on H292 and H23 cell proliferation as assessed by Cell Counting Kit-8 (CCK-8) assays. (d) The percentage of S/G2 population cells was measured by flow cytometry of DHX9 KD H292 and H23 cell lines. (e) Colony formation assays of DHX9 KD H292 and H23 cell lines. Data are shown as the mean ± standard deviation from three independent experiments. *P < 0.05, **P < 0.01, ***P < 0.001. Statistical analysis: Data were performed using unpaired t test (b-e).

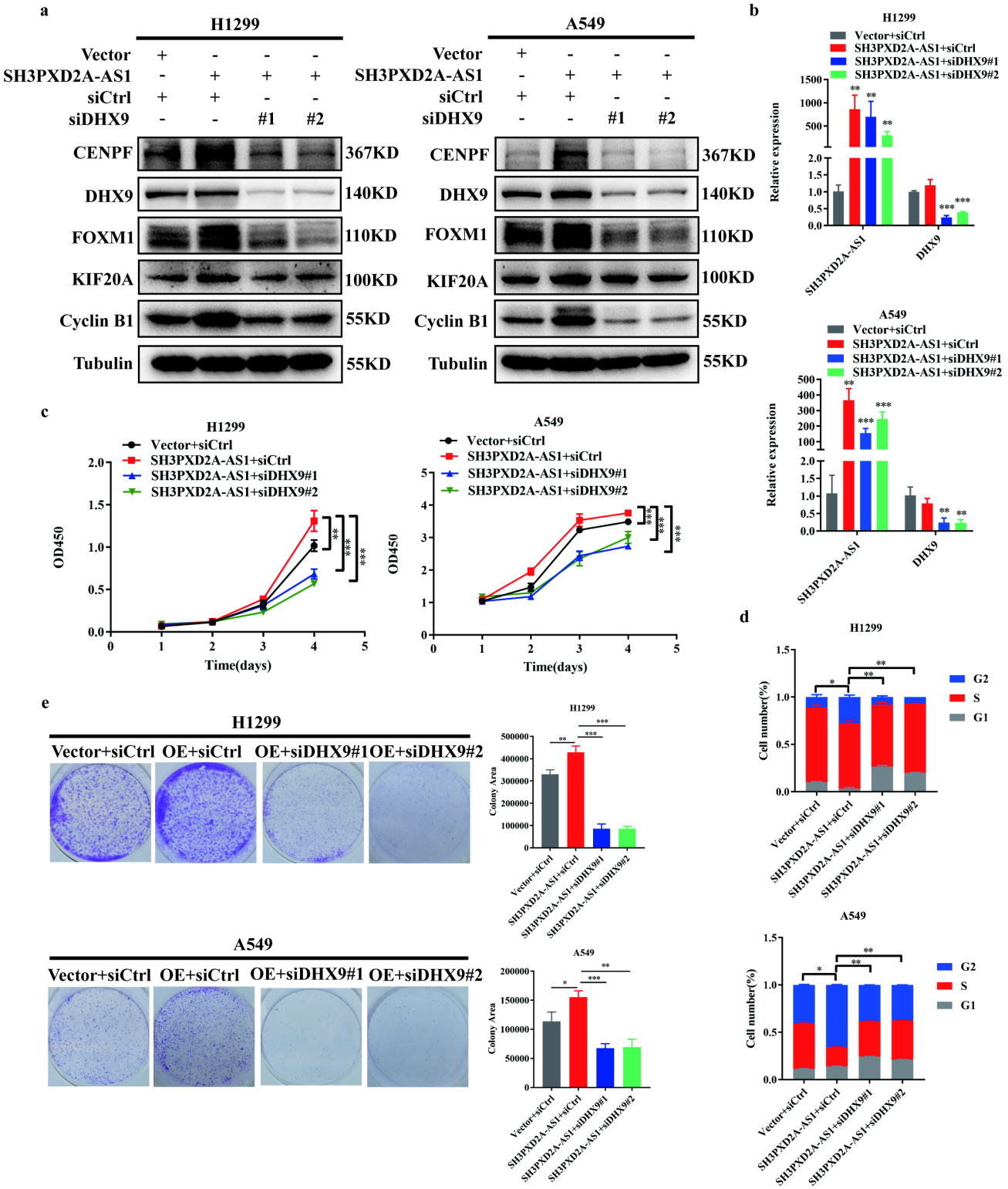

Figure 6

Downregulation of DHX9 reverses the effects on proliferation and cell cycle progression induced by SH3PXD2A-AS1 overexpression. (a) Western blot assays were performed to measure the DHX9, FOXM1, Cyclin B1, KIF20A and CENPF protein levels after transfection of DHX9 siRNA in LINC00460-overexpressing NSCLC cells. (b) qRT-PCR was performed to measure the SH3PXD2A-AS1, DHX9, FOXM1, Cyclin B1, KIF20A and CENPF mRNA levels after transfection of DHX9 siRNA in LINC00460-overexpressing NSCLC cells. (c) Cell Counting Kit-8 (CCK-8) assays for the effects of DHX9 KD on the proliferation of A549 and H1299 cells with SH3PXD2A-AS1 OE. (d) Flow cytometry for the effects of DHX9 KD on the cell cycle of A549 and H1299 cells with SH3PXD2A-AS1 OE. (e) Colony formation assays for the effects of DHX9 KD on the proliferation of A549 and H1299 cells with SH3PXD2A-AS1 OE. Data are shown as the mean ± standard deviation from three independent experiments. *P < 0.05, **P < 0.01, ***P < 0.001. Statistical analysis: Data were performed using unpaired t test (b-e).

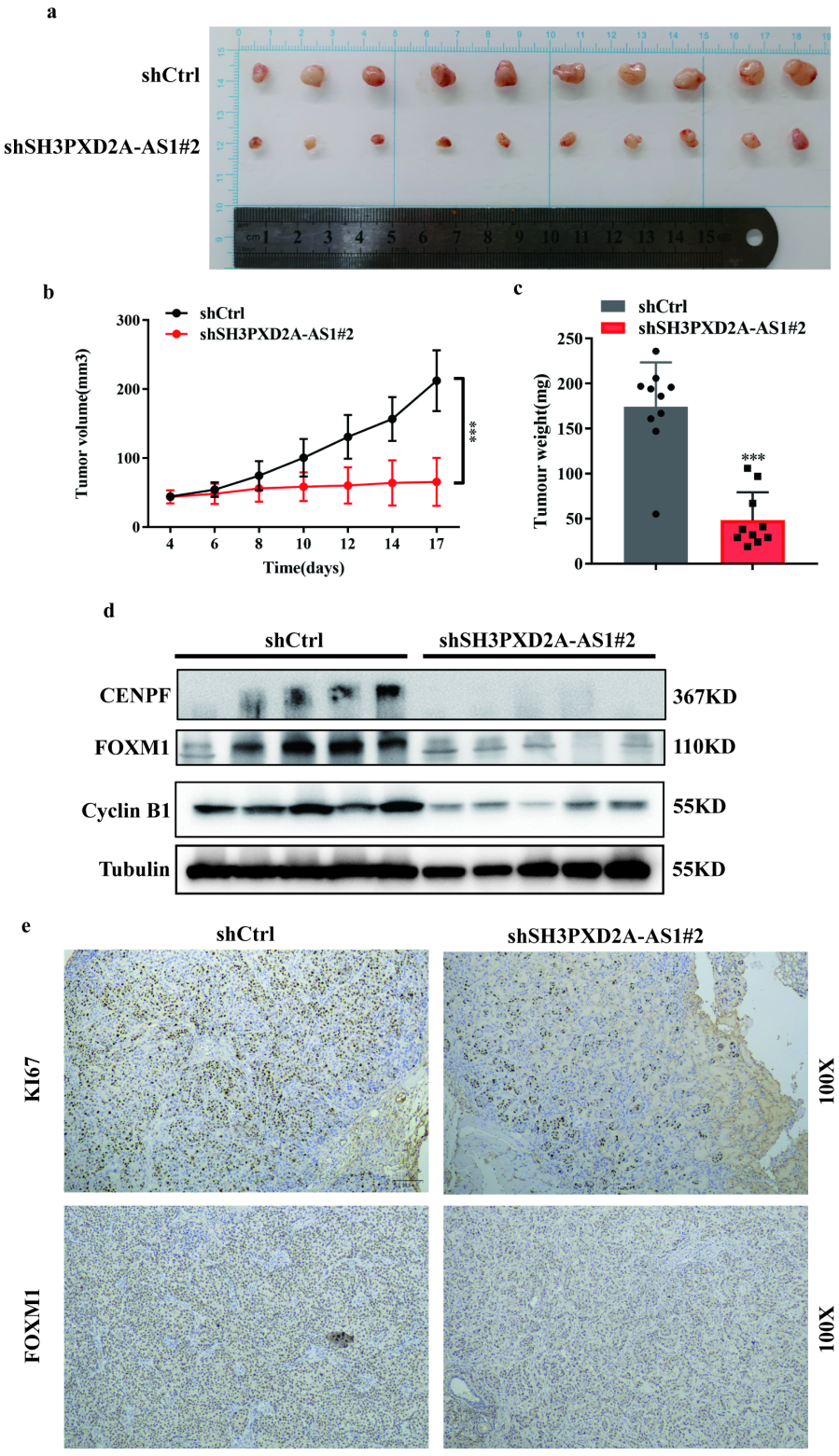

Figure 7

Knockdown of SH3PXD2A-AS1 inhibits NSCLC cell proliferation in vivo. (a, b, c) The effects of SH3PXD2A-AS1 KD on tumour volume and weight were assessed by using the xenograft model. A total of 3×106 H292 SH3PXD2A-AS1 Con/KD cells and Matrigel (Corning; 1:1 ratio) were subcutaneously injected into the flanks of each mouse. ***P<0.001. (d) Western blot analysis of FOXM1, Cyclin B1 and CENPF expression in the tumour xenografts. GAPDH was used as a loading control. (e) The tumour

sections were subjected to immunochemistry staining with antibodies against Ki67 and FOXM1, and representative images are shown. Statistical analysis: Data were performed using unpaired t test (b-c).

Supplementary Files

This is a list of supplementary files associated with this preprint. Click to download.

- SupplementalMaterial.docx
- figureS1.tif
- figureS2.tif